

## Targeted Next Generation Sequencing Identifies Markers of Response to PD-1 Blockade

Douglas B. Johnson<sup>1</sup>, Garrett M. Frampton<sup>6</sup>, Matthew J. Rieth<sup>1,2</sup>, Erik Yusko<sup>7</sup>, Yaomin Xu<sup>3</sup>, Xingyi Guo<sup>3</sup>, Riley C. Ennis<sup>6</sup>, David Fabrizio<sup>6</sup>, Zachary R. Chalmers<sup>6</sup>, Joel Greenbowe<sup>6</sup>, Siraj M. Ali<sup>6</sup>, Sohail Balasubramanian<sup>6</sup>, James X. Sun<sup>6</sup>, Yuting He<sup>6</sup>, Dennie T. Frederick<sup>8</sup>, Igor Puzanov<sup>1</sup>, Justin M. Balko<sup>1,4</sup>, Justin M. Cates<sup>5</sup>, Jeffrey S. Ross<sup>6</sup>, Catherine Sanders<sup>7</sup>, Harlan Robins<sup>7</sup>, Yu Shyr<sup>3</sup>, Vincent A. Miller<sup>6</sup>, Philip J. Stephens<sup>6</sup>, Ryan J. Sullivan<sup>8</sup>, Jeffrey A. Sosman<sup>1</sup>, and Christine M. Lovly<sup>1,4</sup>

### Abstract

Therapeutic antibodies blocking programmed death-1 and its ligand (PD-1/PD-L1) induce durable responses in a substantial fraction of melanoma patients. We sought to determine whether the number and/or type of mutations identified using a next-generation sequencing (NGS) panel available in the clinic was correlated with response to anti-PD-1 in melanoma. Using archival melanoma samples from anti-PD-1/PD-L1-treated patients, we performed hybrid capture-based NGS on 236–315 genes and T-cell receptor (TCR) sequencing on initial and validation cohorts from two centers. Patients who responded to anti-PD-1/PD-L1 had higher mutational loads in an initial cohort (median, 45.6 vs. 3.9 mutations/MB;  $P = 0.003$ ) and a validation cohort (37.1 vs. 12.8 mutations/MB;  $P = 0.002$ ) compared with nonresponders. Response rate, progression-free survival, and overall survival were

superior in the high, compared with intermediate and low, mutation load groups. Melanomas with *NF1* mutations harbored high mutational loads (median, 62.7 mutations/MB) and high response rates (74%), whereas *BRAF/NRAS/NF1* wild-type melanomas had a lower mutational load. In these archival samples, TCR clonality did not predict response. Mutation numbers in the 315 genes in the NGS platform strongly correlated with those detected by whole-exome sequencing in The Cancer Genome Atlas samples, but was not associated with survival. In conclusion, mutational load, as determined by an NGS platform available in the clinic, effectively stratified patients by likelihood of response. This approach may provide a clinically feasible predictor of response to anti-PD-1/PD-L1. *Cancer Immunol Res*; 4(11); 959–67. ©2016 AACR.

### Introduction

Agents targeting the programmed death-1/ligand (PD-1/PD-L1) axis release suppressed antitumor T-cell responses, resulting in remarkable clinical activity in numerous cancers (1). Nivolumab and pembrolizumab induce clinical responses in

25% to 45% of patients with advanced melanoma and are now widely used (2–5). Despite this activity, validated, clinically accessible markers to predict response and to guide treatment decision-making have remained elusive. Clonal expansion of infiltrating T cells and PD-L1 expression by tumor or immune cells is linked with treatment response (2, 4, 6).

Several elegant studies have also demonstrated that a tumor's genomic landscape may influence the efficacy of immune checkpoint inhibitors. Specifically, greater numbers of somatic mutations and resultant tumor neoantigens correlate with therapeutic benefit in melanoma (with ipilimumab; refs. 7, 8), in non-small cell lung cancer (NSCLC; refs. 9, 10), and mismatch-repair-deficient tumors (with pembrolizumab; ref. 11). Other studies have suggested that mutations or aberrant signaling in particular oncogenes modulate antitumor immune responses (12–15).

Despite these compelling studies, the impact of mutational load [number of point mutations per megabase (MB) of DNA] and specific oncogenic mutations on response to anti-PD-1 in melanoma has not been systematically explored and validated. Furthermore, translating these findings to routine clinical practice remains problematic as whole-exome sequencing (WES) is expensive, time-intensive, and technically challenging. Profiling a smaller fraction of the genome (>1 MB; approximately 3% of the exome) using an extensively validated hybrid capture-based next-generation sequencing (NGS) diagnostic platform (FoundationOne; ref. 16) could serve as a useful surrogate for total mutational load and identify particular mutations that correlate with

<sup>1</sup>Department of Medicine, Vanderbilt University Medical Center and Vanderbilt Ingram Cancer Center, Nashville, Tennessee. <sup>2</sup>Department of Bioinformatics, Vanderbilt University Medical Center and Vanderbilt Ingram Cancer Center, Nashville, Tennessee. <sup>3</sup>Department of Biostatistics, Vanderbilt University Medical Center and Vanderbilt Ingram Cancer Center, Nashville, Tennessee. <sup>4</sup>Department of Cancer Biology, Vanderbilt University Medical Center and Vanderbilt Ingram Cancer Center, Nashville, Tennessee. <sup>5</sup>Department of Pathology, Vanderbilt University Medical Center and Vanderbilt Ingram Cancer Center, Nashville, Tennessee. <sup>6</sup>Foundation Medicine Inc., Cambridge, Massachusetts. <sup>7</sup>Adaptive Biotechnologies, Seattle, Washington. <sup>8</sup>Department of Medicine, Massachusetts General Hospital, Boston, Massachusetts.

J.A. Sosman and C.M. Lovly contributed equally to this article and share senior authorship.

**Note:** Supplementary data for this article are available at Cancer Immunology Research Online (<http://cancerimmunolres.aacrjournals.org/>).

**Corresponding Author:** Douglas B. Johnson, Vanderbilt University Medical Center, 777 PRB, 2220 Pierce Ave, Nashville, TN 37232. Phone: 205-317-3791; Fax: 615-343-7602; E-mail: Douglas.b.johnson@vanderbilt.edu

**doi:** 10.1158/2326-6066.CIR-16-0143

©2016 American Association for Cancer Research.

response to anti-PD-1/PD-L1. Integrating immune microenvironment profiling through T-cell receptor (TCR) NGS (ImmunoSeq) to quantify T-cell infiltration and clonality could further enhance biomarker approaches. Ultimately, we hypothesized that these specialized NGS approaches would provide clinically useful predictors of response to anti-PD-1/PD-L1 in patients with advanced melanoma.

## Patients and Methods

### Patients

Protected health information was reviewed according to Health Insurance Portability and Accountability Act (HIPAA) guidelines. Patient samples were retrospectively selected under IRB-approved protocols. Patients had metastatic melanoma and began anti-PD-1 (nivolumab or pembrolizumab) or anti-PD-L1 (atezolizumab) between January 2011 and March 2015 through clinical trials or standard therapy. All patients had evaluable responses determined by radiographic imaging or had rapid clinical progression precluding further imaging. Cross-sectional imaging was performed at 8- to 12-week intervals per study protocols or standard of care. Baseline characteristics, treatment response, progression-free survival (PFS), and overall survival (OS) were obtained through medical record and tumor imaging review. Patients were classified as responders if they experienced partial or complete responses by RECIST 1.1 (ref. 17;  $n = 30$ ) or atypical immune-related responses lasting  $\geq 12$  months ( $n = 2$ ), or as nonresponders if they failed to respond ( $n = 33$ ).

Biopsies or resection samples were obtained from the Vanderbilt University Medical Center and Massachusetts General Hospital. Most formalin-fixed paraffin embedded (FFPE) specimens underwent FoundationOne for research purposes only ( $n = 40$ ). These samples comprised all patients with remaining available FFPE with evaluable therapeutic responses at the time of the analysis. All Vanderbilt patients treated with anti-PD-1/PD-L1 that obtained FoundationOne for clinical purposes (e.g., to identify actionable mutations;  $n = 25$ ) were also included. Most samples were obtained within 12 months prior to starting treatment ( $n = 43$ ). Other specimens were obtained  $> 12$  months before therapy ( $n = 15$ ) or even shortly after treatment initiation ( $n = 7$ ). All pretreatment samples with available tissue underwent ImmunoSeq strictly for research purposes.

### NGS and The Cancer Genome Atlas (TCGA) analysis

DNA sequencing was performed using an extensively validated, Clinical Laboratory Improvement Amendments–certified, hybrid capture–based NGS platform (FoundationOne, Foundation Medicine; ref. 16). The initial cohort ( $n = 32$ ) was sequenced by a version used between December 2012 and August 2014, which evaluated exons from 236 cancer-related genes and introns of 19 genes. An independent validation cohort ( $n = 33$ ) was sequenced using a subsequent version used since August 2014 comprising exons from 315 genes and introns from 28 genes. Methods for DNA extraction and sequencing have been extensively validated and published (16).

To calculate total mutational burden, we quantified the number of somatic mutations detected on the FoundationOne test and extrapolated that value to the whole exome using the following algorithm. All detected short variant alterations, base substitutions, and indels were counted. All coding alterations, including silent alterations, were also counted, whereas noncoding altera-

tions were excluded. Alterations with known (occurring as known somatic alterations in the COSMIC database; <http://cancer.sanger.ac.uk/cosmic>) and likely (truncations in tumor suppressor genes) functional status were not counted. This correction was performed to avoid upward skewing of mutational load, because FoundationOne preferentially profiles genes known to be recurrently mutated in cancer. Predicted germline variants were excluded and filtered using the dbSNP database (<http://www.ncbi.nlm.nih.gov/SNP/>), the ExAC database (those with  $\geq 2$  counts; <http://exac.broadinstitute.org/>), and the SGZ (somatic germline zygosity) algorithm (unpublished observations). The SGZ algorithm was refined using  $>60,000$  Foundation Medicine specimens to further reduce the chance of calling germline variants. To calculate the mutation load per MB, the total number of mutations counted was divided by the coding region target territory, covering 0.91 and 1.25 MB for the 236 gene and 315 gene versions, respectively.

We retrieved matched somatic mutation and clinical data from 345 skin cutaneous melanoma tumor samples from TCGA (including 263 with clinical data) from the CbioPortal (<http://www.cbioportal.org/public-portal/>) using the Cancer Genome Data Server-R (CGDS-R) API, which provided a set of functions for extracting data from the CGDS. Using TCGA, we compared the number of nonsynonymous mutations in 315 genes sequenced in FoundationOne to total mutations identified by all coding genes by WES ( $n = 20,022$ ). We also evaluated survival data for these samples.

### T-cell Receptor Sequencing

TCR sequencing and clonality quantification, and determination of T-cell fraction, were assessed in pretreatment FFPE tumor samples using survey level ImmunoSeq, as previously described (Adaptive Biotechnologies; refs. 6, 18). T-cell clonality was calculated as follows: Shannon entropy was calculated on the clonal abundance of all productive TCR sequences in the data set. Shannon entropy was normalized by dividing Shannon entropy by the logarithm of the number of unique productive TCR sequences. This normalized entropy value was then inverted ( $1 - \text{normalized entropy}$ ) to produce the clonality metric.

### Statistical analysis

Mutational load was compared between responders and nonresponders using the Mann–Whitney  $U$  test. The performance of mutational load across a range of values was calculated, and thresholds for the low, intermediate, and high groups were selected from local maxima across a range of clinically meaningful values using ROC curves. ROC was used to identify the optimal mutation cutoffs from the initial cohort to assess in the validation cohort. Response rates between patients with particular genomic changes were compared using  $\chi^2$  testing and were not corrected for multiple comparisons. T-cell clonality and T-cell fraction were compared between responders and nonresponders using the Mann–Whitney  $U$  test. In the TCGA samples, mutation number identified in 315 FoundationOne genes was correlated with all coding genes ( $n = 20,022$ ) using the Spearman test (19). Survival in the TCGA was also correlated with mutational load calculated by WES and FoundationOne genes, and compared between mutational load groups using Cox proportional hazards. PFS and OS were assessed by Kaplan–Meier and patients were censored at last follow-up, if progression-free and/or alive. PFS and OS for high, intermediate, and low mutation load groups were compared using the log-rank

**Table 1.** Clinical characteristics of the initial and validation cohorts

Variable	Initial cohort (n = 32) Number (%)	Validation cohort (n = 33) Number (%)	P
Age (median, range)	55 (33–80)	62 (32–85)	0.65
Sex			
Male	21 (66)	17 (52)	0.25
Female	11 (34)	16 (48)	
Metastatic stage			
IV M1a	3 (9)	2 (6)	0.79
IV M1b	5 (16)	4 (12)	
IV M1c	24 (75)	27 (82)	
Primary tumor site			
Cutaneous	18 (56)	26 (79)	0.13
Non-cutaneous	10 (31)	4 (12)	
Unknown	4 (13)	3 (9)	
Treatment			
Nivolumab	15	4	<0.001
Pembrolizumab	14	29	
Atezolizumab	3	0	
Prior therapy			
Lines of prior therapy (median, range)	1 (0–4)	1 (0–6)	0.23
Prior BRAF inhibitor	3 (9)	8 (24)	0.11
Prior ipilimumab	14 (44)	23 (70)	0.03
Prior chemotherapy	5 (16)	5 (15)	0.96

test. Cox proportional hazards analysis was performed to assess the impact of mutation load, controlled for stage, age, gender, and prior ipilimumab. All analyses were performed using GraphPad Prism version 6.05 and R version 3.2.1.

## Results

### Mutational load by hybrid capture–based NGS correlates with anti–PD-1/PD-L1 response

We performed hybrid capture–based NGS in samples from patients treated with anti–PD-1/PD-L1 (Table 1). In an initial cohort, the mutation load in anti–PD-1/PD-L1 responders was significantly greater than in nonresponders (median, 45.6 vs. 3.9 mutations/MB;  $P = 0.003$ , Fig. 1A). We observed a similar difference in the validation cohort (median, 37.1 vs. 12.8 mutations/MB,  $P = 0.002$ ; Fig. 1B). Results were similar in "optimal" samples obtained within 12 months of starting treatment compared with all other samples (Supplementary Table S1).

We then assessed whether particular cutoffs could be used to classify patients by likelihood of response to therapy. Using optimized ROC on the initial cohort, it appeared that stratifying patients into three groups had superior performance compared with binary classification (Supplementary Fig. S1A and S1B). We thus divided patients into high (>23.1 mutations/MB), intermediate (3.3–23.1 mutations/MB), and low (<3.3 mutations/MB) mutation load groups. Using these thresholds, we observed superior objective response rates (ORR) in the high mutational load group, followed by intermediate and low groups (82% vs. 36% vs. 10% response rate;  $\chi^2 P = 0.003$ ; Table 2). In the validation cohort, superior ORR also occurred in the high mutation load group (88% vs. 29% vs. 25%,  $\chi^2 P = 0.001$ ). Aggregating both cohorts, the ORR was greatest in high (85%) followed by intermediate (29%) and low (14%) mutation load groups ( $P < 0.001$ ).

We then evaluated other clinical outcomes. Across both cohorts, PFS correlated with mutation load; superior PFS was observed in the high mutation load group compared with the intermediate and low groups (median not reached vs. 89 days vs.

86 days,  $P < 0.001$ ; Fig. 1C). OS followed a similar pattern (median not reached vs. 300 days vs. 375 days;  $P < 0.001$ ; Fig. 1D). Although ORR seemed higher in the intermediate than in the low mutation load group, PFS and OS appeared similar between these groups. High mutation load was also associated with superior OS and PFS using Cox proportional hazards model, adjusted for age, gender, stage, and prior ipilimumab (high vs. low HR, 0.14,  $P < 0.001$  for PFS; HR, 0.09,  $P < 0.001$  for OS; Supplementary Tables S2 and S3).

Non-cutaneous melanomas (including acral subtype) have far fewer mutations than those of cutaneous origin, and perhaps less frequent responses to immunotherapy, whereas the mutational profile of melanomas of unknown origin mirrors cutaneous melanomas (20–22). To exclude confounding from non-cutaneous melanomas, we assessed mutational load in melanomas of cutaneous/unknown origin separately and observed a higher mutational load in responders (median, 39.0 vs. 14.4 mutations/MB,  $P < 0.001$ ; Supplementary Fig. S2A). No difference in mutational load was identified in 14 patients (albeit with only 2 responders) in patients with non-cutaneous melanomas (median, 4.5 vs. 2.2 mutations/MB,  $P = 0.714$ ; Supplementary Fig. S2B).

Next, we assessed whether particular types of genomic changes correlated with response. Total identified mutations (including those with known or likely functional significance) were strongly associated with response (median, 46.5 vs. 6.0 mutations,  $P < 0.001$ ; Fig. 2A). C>T transitions (associated with ultraviolet radiation damage) were more numerous in responders (median 33.5 vs. 3.0 transitions,  $P < 0.001$ ; Fig. 2B). Most other nucleotide variants also occurred more commonly in responders, albeit at lower frequencies (Fig. 2C). By contrast, gene amplifications and deletions were similar between groups (Supplementary Fig. S2C).

We then investigated whether mutational load differed between particular "driver mutation"–defined subsets. We observed marked differences among *BRAF*, *NRAS*, *NF1*, and "triple WT" (wild-type) melanomas (median, 12.0 vs. 17.6 vs. 62.7 vs. 2.2 mutations/MB, respectively;  $P < 0.001$ ; Fig. 2D). Notably, melanomas with *NF1* mutations have been linked with chronic ultraviolet light damage and high mutational loads previously (19, 20). By contrast, the "triple WT" group harbored an extremely low mutational load.

To determine whether mutation load in these 236 to 315 genes could serve as a robust correlate for total genomic mutational load as assessed by WES, we evaluated 345 archival TCGA samples (19). The total number of mutations identified in these genes strongly correlated with total exome mutation number ( $R = 0.995$ ,  $P < 0.001$ ; Fig. 3A). This correlation appeared particularly robust in samples with high mutational loads. To assess whether mutational load associated with improved outcomes in unselected patients (not receiving anti–PD-1/PD-L1), we assessed survival among TCGA samples with evaluable survival data ( $n = 263$ ). No significant correlation was observed using the FoundationOne genes ( $P = 0.14$ ) or WES ( $P = 0.06$ ). Using our three mutation load groups, patients with intermediate mutational load experienced the longest survival (HR = 2.1 for intermediate vs. low,  $P = 0.008$ ; Fig. 3B and C).

### Specific mutations and response to anti–PD-1/PD-L1

Next, we assessed mutations in particular cancer-related genes to assess their impact on response to anti–PD-1. We limited this analysis to previously described functional alterations and excluded variants of unknown significance (VUS) unless noted. We

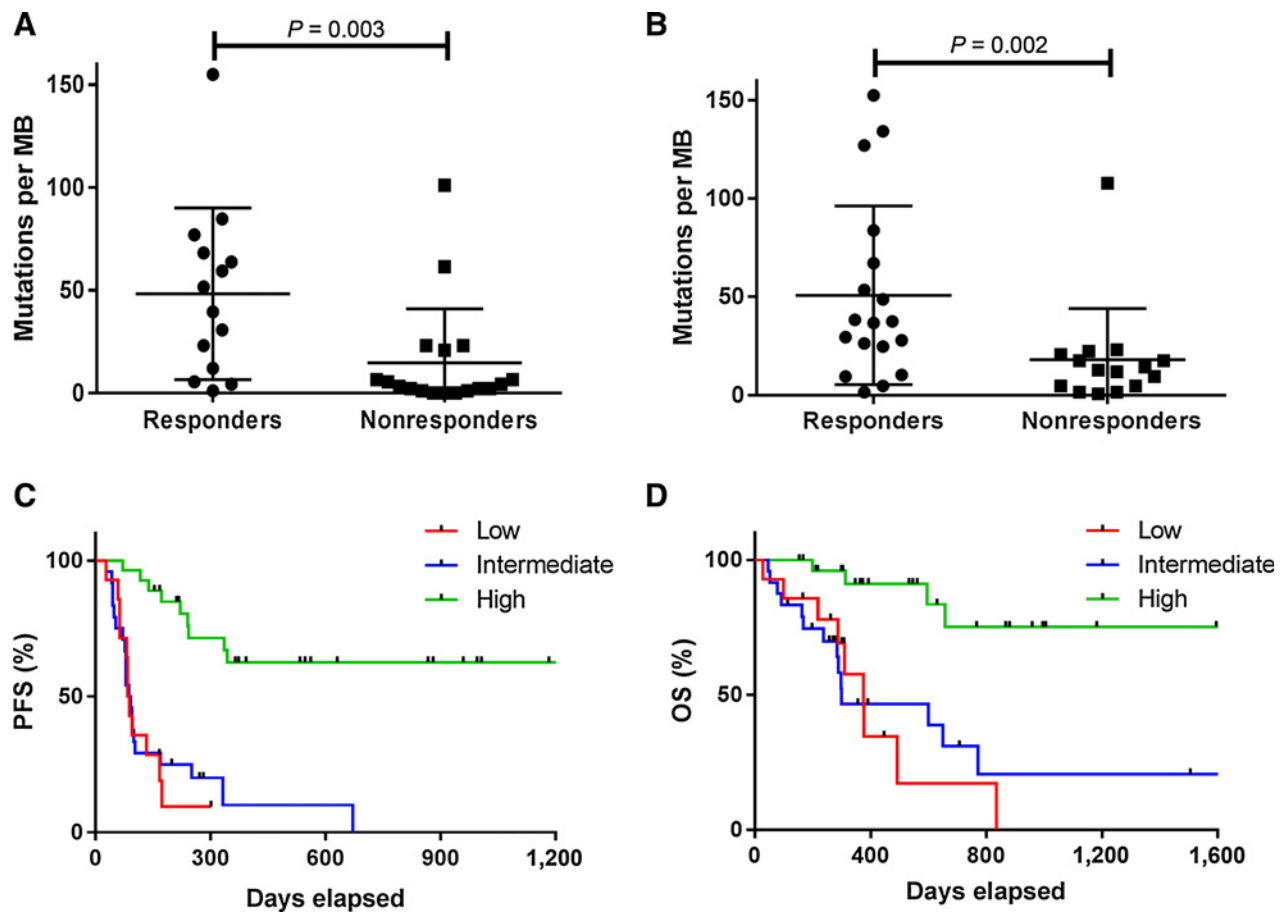


**Figure 1.** Mutational load in responders versus nonresponders in initial cohort (A) and validation cohort (B). Progression-free survival (C) and overall survival (D) in patients with high, intermediate, and low mutational load.

identified several genes that were more frequently altered in responders or nonresponders (Table 3; Fig. 4). Some genomic alterations correlated with mutational load; for example, *NF1* alterations were more common in responders (50% vs. 21%,  $P = 0.015$ ; ORR 74%), whereas "triple WT" patients were more often in the nonresponding group (13% vs. 35%,  $P = 0.045$ ). In smaller numbers, we did not observe that responses correlated with gene alterations previously linked to immunotherapy response (*NRAS*; ref. 12), T-cell exclusion (*CTNNB1*; ref. 14),

or PD-L1 regulation (*MYC*; ref. 15). Loss of *PTEN* has been linked to PD-L1 expression (in glioblastoma) and immunosuppressive cytokine profiles (in melanoma; ref. 13). Although both patients with *PTEN* loss failed to respond, we did not observe a significant difference in the incidence of *PTEN*-inactivating mutations when comparing responders with nonresponders (13% vs. 15%,  $P = 0.76$ ). *MYC* amplification appeared to be more common in nonresponders, but conclusions were limited by sample size. *BRCA2* mutations (including

**Table 2.** Response rate stratified by mutational burden

	Response	No response	P
<b>Initial cohort (n = 32)</b>			
High (>23.1 mutations/MB), n = 11	9 (82%)	2 (18%)	0.003
Intermediate (3.3-23.1 mutations/MB), n = 11	4 (36%)	7 (64%)	
Low (<3.3 mutations/MB), n = 10	1 (10%)	9 (90%)	
<b>Validation cohort (n = 33)</b>			
High (>23.1 mutations/MB), n = 16	14 (88%)	2 (12%)	0.001
Intermediate (3.3-23.1 mutations/MB), n = 13	3 (23%)	10 (77%)	
Low (<3.3 mutations/MB), n = 4	1 (25%)	3 (75%)	
<b>Entire cohort (n = 65)</b>			
High (>23.1 mutations/MB), n = 27	23 (85%)	4 (15%)	<0.001
Intermediate (3.3-23.1 mutations/MB), n = 24	7 (29%)	17 (71%)	
Low (<3.3 mutations/MB), n = 14	2 (14%)	12 (86%)	

Downloaded from <http://aacrjournals.org/cancerimmunolres/article-pdf/4/11/959/2349864/959.pdf> by guest on 06 August 2024

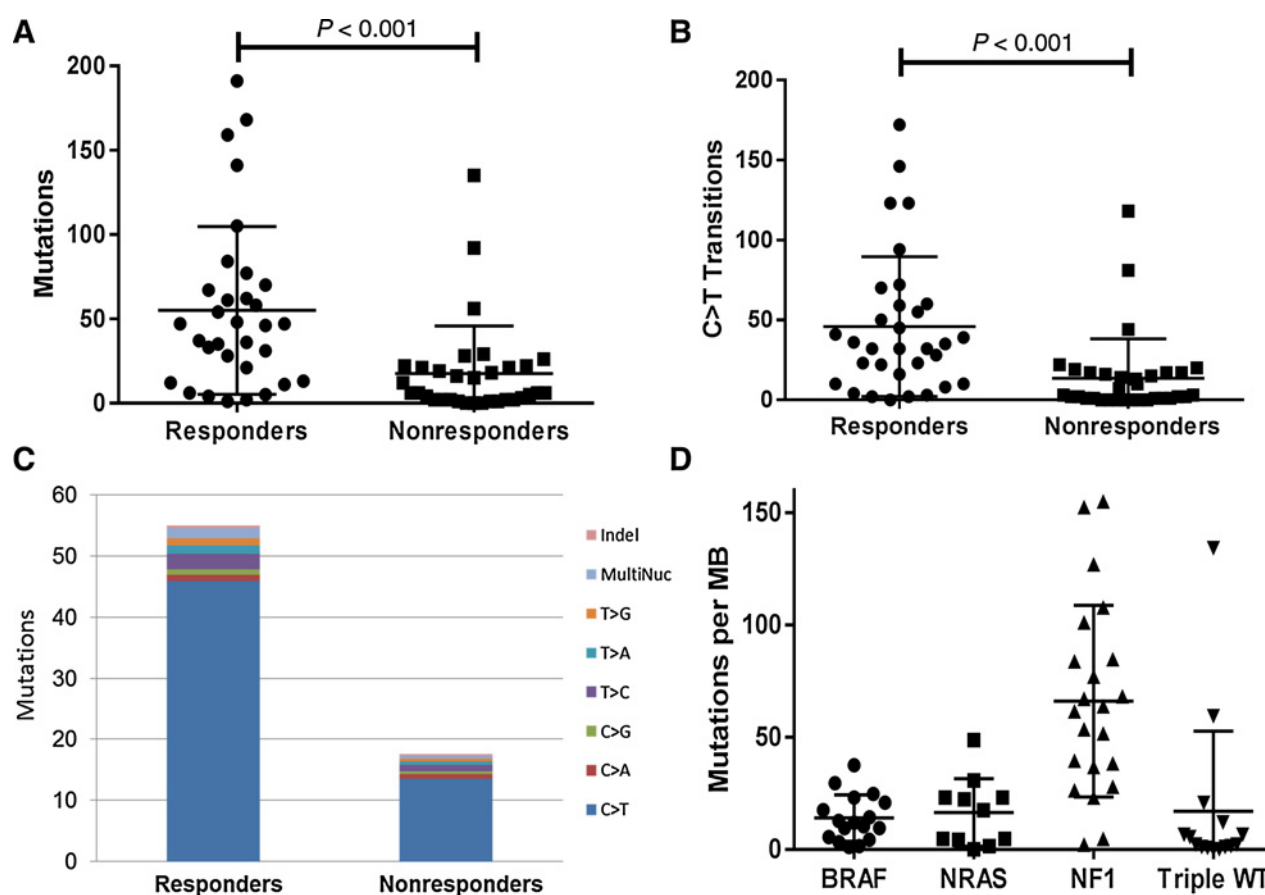


**Figure 2.**

Genetic alterations observed in responders versus nonresponders: **A**, total number of mutations; **B**, total number of C>T transitions; **C**, types of nucleotide substitutions; **D**, mutational load of patients with *BRAF* mutations, *NRAS* mutations, *NF1* mutations/loss, and "triple WT" (defined as wild-type for *BRAF*, *NRAS*, and *NF1*). *BRAF* non-V600 mutations were included with in the *BRAF* cohort except for 1 patient with concurrent *NF1* mutation. One patient with *NRAS*<sup>G61R</sup> mutation and concurrent *NF1* mutation was included in the *NRAS* cohort.

VUS) appeared more common in responders (5 of 32) compared with nonresponders (2 of 33); melanomas with *BRCA2* mutations had higher mutational load than those lacking these mutations (median, 68.2 vs. 15.9 mut/MB;  $P = 0.028$ ; ref. 23).

#### *LRP1B* mutations and total mutation load

We also observed frequent mutations in *LRP1B*. This putative tumor suppressor is a large, 1.9-MB gene designated a common fragile site (region of profound genomic instability; ref. 24). We speculated that mutations detected herein might serve as a single-gene surrogate for total mutational load and response (a "barometer" of total exonic mutational load). Among responders, 11 patients harbored *LRP1B* mutations compared with 1 nonresponder (34% vs. 3%,  $P = 0.008$ ). When extended to VUS, responders had on average 2.8 mutations/VUS compared with 0.9 for nonresponders ( $P = 0.016$ ; Supplementary Fig. S3A); 75% of responders had  $\geq 1$  mutation/VUS compared with 38% of nonresponders ( $P = 0.002$ ). In TCGA samples (19), melanomas with *LRP1B* mutations had significantly more mutations compared with those lacking *LRP1B* mutations (median, 542 vs. 219,  $P < 0.001$ ; Supplementary Fig. S3B), and mutational load correlated with number of *LRP1B* muta-

tions per tumor (Spearman  $R = 0.54$ ,  $P < 0.001$ ; Supplementary Fig. S3C). Although it remains unclear whether *LRP1B* mutations have intrinsic immune effects, these data suggest that sequencing even a single, frequently mutated gene may provide insight into genome-wide mutational load and even correlate with anti-PD-1 responses.

#### TCR clonality does not correlate with clinical benefit or mutational load

We then investigated whether T-cell infiltration and clonality correlated with mutational load and could enhance the predictive capacity of this approach by performing TCR NGS in available tumor samples ( $n = 42$ ). Increased clonality (and decreased diversity) of the TCR  $\beta$ -chain repertoire may indicate preexisting infiltration of tumor-specific antigen populations and has been linked with response to anti-PD-1 (6). However, we observed that TCR clonality did not correlate with response to anti-PD-1 (median, 0.11 vs. 0.11,  $P = 0.54$ ; Supplementary Fig. S4A). Furthermore, T-cell fraction did not correlate with response (median, 0.13 vs. 0.09,  $P = 0.11$ ; Supplementary Fig. S4B). Since time or intervening therapies may modulate TCR clonality/T-cell infiltration, we assessed a subset of samples obtained within

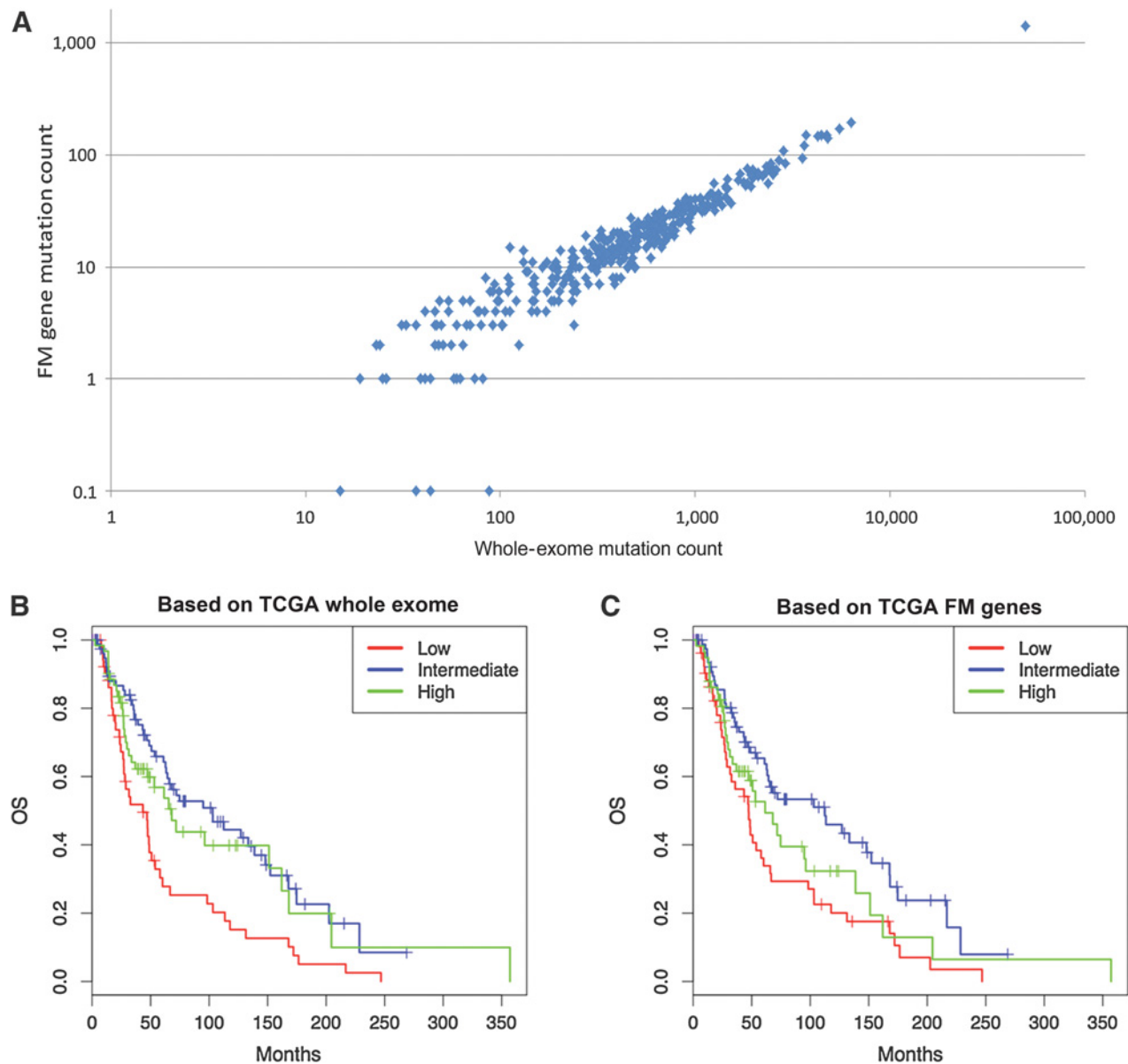


**Figure 3.**

**A**, mutational load in TCGA skin cutaneous melanoma (SKCM) samples using 315 genes included on the hybrid capture NGS panel is highly correlated with mutations assessed by WES. Mutational load groups and survival in the TCGA using **(B)** WES and **(C)** 315 FoundationOne (FM) genes. For low, intermediate, and high mutation load groups, we observed a difference in OS using WES (median, OS 43.4 months vs. 103.0 months vs. 68.0 months,  $P = 0.001$ ) and FM genes (median, 47.3 vs. 112.5 months vs. 61.5 months,  $P = 0.008$ ).

4 months of starting anti-PD-1 without interval therapies. Among this group ( $n = 14$ ), we observed nonstatistically significant trends to increasing clonality and T-cell fraction among responders (Supplementary Fig. S4C/D; ref. 6). T-cell clonality and T-cell fraction also did not correlate with mutational load (Supplementary Fig. S5).

## Discussion

The development of anti-PD-1/PD-L1 agents has revolutionized therapeutic strategies for melanoma and many other cancers.

In this study, we found that mutation number as detected by a several-hundred gene hybrid capture-based NGS platform strongly correlated with benefit from anti-PD-1/PD-L1. Here, we demonstrated and validated the link between anti-PD-1 responses and mutation load in melanoma (the elegant study by Hugo and colleagues assessed a single cohort of 38 patients; ref. 23). In particular, stratifying patients into "high," "intermediate," and "low" mutation load cohorts provided a clinically feasible marker of response to anti-PD-1/PD-L1 in advanced melanoma.

Total mutational load has been linked with benefit from immune checkpoint inhibitors in several cancers (7–11, 23).

**Table 3.** Altered genes in responders and nonresponders

Gene	Responders	Nonresponders	P
	(n = 32) Number (%)	(N = 33) Number (%)	
<i>BRAF</i> V600	5 (16)	9 (27)	0.25
<i>BRAF</i> non-V600	3 (9)	1 (3)	0.29
<i>NRAS</i>	5 (16)	6 (18)	0.78
<i>NF1</i>	16 (50)	7 (21)	0.02
"Triple WT" <sup>a</sup>	4 (13)	11 (33)	0.05
<i>TP53</i>	9 (28)	7 (21)	0.57
<i>MYC</i>	2 (6)	4 (12)	0.41
<i>APC/CTNNB1</i>	3 (9)	2 (6)	0.61
<i>IGF1R/HGF</i>	4 (13)	2 (6)	0.37
<i>PTEN</i>	4 (13)	5 (15)	0.76
<i>CDKN2A/CDK4/CDK6/RB1</i> alterations	14 (44)	19 (58)	0.27
<i>LRP1B</i>	11 (34)	1 (3)	0.001

<sup>a</sup>*BRAF*, *NRAS*, *NF1* wild-type.

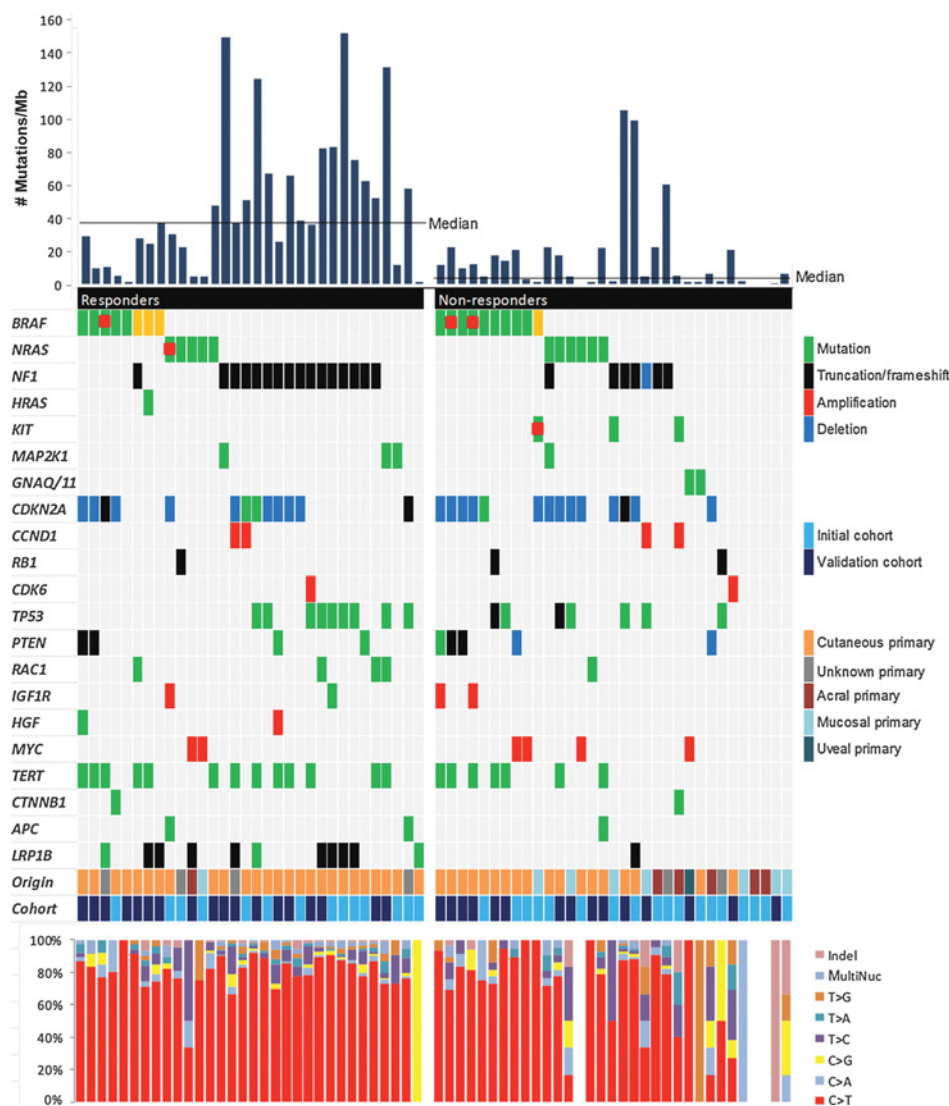
Under the current understanding, the likelihood of generating immunogenic tumor neoantigens rises in a probabilistic fashion as mutations develop, increasing the likelihood of immune

recognition (25). Assessing total mutational load, however, requires WES. This approach necessitates specialized tissue processing, matched normal specimen, and is largely performed as a research tool. Given the technical and informatics challenges of performing WES in clinical settings, surrogate methods of detecting mutational load are needed. This validated hybrid capture-based NGS platform has several pragmatic advantages, including clinically feasible turnaround times (~2 weeks), standardized informatics pipelines, and manageable (although still considerable) costs. This approach has other potential advantages over subjective, immunohistochemistry markers such as PD-L1 expression, because it produces an objective measure (26). Finally, this platform facilitates simultaneous detection of actionable alterations relevant for targeted therapy selection.

Augmenting this analysis with TCR sequencing did not enhance the response prediction in this dataset. In view of the dynamic nature of the antitumor immune response, we speculate that these archival tumor samples may not capture an accurate view of the pretreatment tumor microenvironment. A prior study using fresh

**Figure 4.**

Top, calculated mutational load per sample. Middle, color-coded matrix of individual mutations, copy-number alterations, and clinical characteristics. Bottom, mutation spectra of individual samples.



Downloaded from <http://aacrjournals.org/cancerimmunolres/> article-pdf/4/1/1959/2349864/959.pdf by guest on 06 August 2024

biopsies demonstrated that TCR clonality correlated with treatment responses (6). Indeed, in a subset of samples approximating this context, a similar but nonsignificant trend was observed, suggesting TCR clonality is most predictive directly prior to treatment.

Identifying accurate predictive biomarkers for anti-PD-1/PD-L1 therapy has several clinical applications. In melanoma, one could foresee that patients with high mutational load could receive anti-PD-1 monotherapy, whereas those with intermediate/low mutational loads could be treated with the more active (but more toxic) combination of nivolumab and ipilimumab (5). In other malignancies (e.g., NSCLC) with a lower response rate to anti-PD-1, this approach could potentially stratify patients between anti-PD-1 and cytotoxic chemotherapy. High mutation loads defined by this assay correlated with therapeutic responses in urothelial bladder cancer patients treated with atezolizumab (27). No differences in survival were noted between the "intermediate" and "low" mutation load groups in our paper, which could imply that a "threshold effect" may be present, and that the effect on response and survival may be most pronounced in the "high" mutation load group.

Alterations in several genes correlated with benefit from anti-PD-1. Although certain genetic changes may directly influence the immune microenvironment as shown by others (13–15), our findings suggest that other alterations may simply correlate with or contribute to increased mutational load (e.g., *NF1*, *LRP1B*, and *BRCA2*). Given the relatively low incidence of many of these events (e.g., *PTEN* loss, *MYC* amplification, and *CTNNB1* mutations/deletions), much larger datasets will be needed to assess the effects of these genetic changes on response to therapy. Alternatively, RNA sequencing/gene expression data may also augment these analyses.

Our study has several limitations. First, archival samples were used, rather than uniformly timed biopsies performed strictly for research. The archival nature of these samples, however, more closely resembles "real-world" clinical practice and suggests that this approach may be clinically feasible. Second, the sample size was not adequate to make conclusions about rarer genomic alterations. Third, no matched control group was available to determine whether mutation load is truly predictive versus prognostic. However, overall mutation load and survival were not correlated in our analysis of unselected samples from the TCGA, arguing for an anti-PD-1-specific effect. Finally, no matched normal tissue was sequenced to conclusively rule out all germline polymorphisms, although an algorithm incorporating numerous available tools excluded the vast majority of germline alterations. Further, the overwhelming proportion of C>T transitions (characteristic of, although not entirely specific for, UV light-induced DNA damage) mirroring WES studies argues that this represents an accurate surrogate even without 100% certainty on every variant call.

In conclusion, mutational load in advanced melanoma as determined by hybrid capture-based NGS strongly correlated with response to anti-PD-1/PD-L1 therapy in two independent cohorts. This was especially marked in the "high" mutational load group, which comprised >40% of studied samples. We suggest that testing of mutational load by this rigorously validated approach can improve treatment decision-making, allow more

rational use of costly agents, and enhance this new era of precision immunotherapy.

### Disclosure of Potential Conflicts of Interest

D.B. Johnson is a consultant/advisory board member for BMS and Genoptix. G.M. Frampton is employed at Foundation Medicine and has ownership interest (including patents) in the same. E. Yusko is a senior computational biologist at Adaptive Biotechnologies. R.C. Ennis is co-founder and COO of Freenome and Oncolinx and co-founder, CEO of Immudicon, and has ownership interest (including patents) in Freenome, Immudicon, and Oncolinx. D. Fabrizio is leader, cancer immunotherapy at Foundation Medicine, Inc. Z.R. Chalmers, J. Greenbowe, and S.M. Ali have ownership interest (including patents) in Foundation Medicine, Inc. S. Balasubramanian is Senior Manager, Strategic Alliances at Foundation Medicine and has ownership interest (including patents) in the same. J.X. Sun is a scientist at Foundation Medicine and has ownership interest (including patents) in the same. I. Puzanov is a consultant/advisory board member for Amgen and Roche. J.M. Balko reports receiving a commercial research grant from Incyte. J.S. Ross reports receiving a commercial research grant from Foundation Medicine and has ownership interest (including patents) in the same. H. Robins is CSO at Adaptive Biotechnologies and has ownership interest (including patents) in the same. V. Miller is chief medical officer at Foundation Medicine, Inc. P.J. Stephens is CSO at Foundation Medicine, Inc. and has ownership interest (including patents) in the same. C.M. Lovly reports receiving a commercial research grant from Novartis, Astra Zeneca, and Xcovery is a consultant/advisory board member for Ariad, Novartis, Clovis, Sequenom, and Genoptix. No potential conflicts of interest were disclosed by the other authors.

### Authors' Contributions

**Conception and design:** D.B. Johnson, G.M. Frampton, R.C. Ennis, D. Fabrizio, J.S. Ross, C. Sanders, H. Robins, R.J. Sullivan, J.A. Sosman, C.M. Lovly

**Development of methodology:** D.B. Johnson, G.M. Frampton, R.C. Ennis, D. Fabrizio, Z.R. Chalmers, J.X. Sun, Y. He, J.S. Ross, H. Robins

**Acquisition of data (provided animals, acquired and managed patients, provided facilities, etc.):** D.B. Johnson, G.M. Frampton, Z.R. Chalmers, S.M. Ali, D.T. Frederick, I. Puzanov, J.M. Cates, J.S. Ross, R.J. Sullivan, J.A. Sosman

**Analysis and interpretation of data (e.g., statistical analysis, biostatistics, computational analysis):** D.B. Johnson, G.M. Frampton, M.J. Rieth, E. Yusko, Y. Xu, X. Guo, R.C. Ennis, D. Fabrizio, Z.R. Chalmers, J. Greenbowe, J.X. Sun, J.M. Balko, J.S. Ross, C. Sanders, Y. Shyr, V.A. Miller, J.A. Sosman, C.M. Lovly

**Writing, review, and/or revision of the manuscript:** D.B. Johnson, G.M. Frampton, M.J. Rieth, E. Yusko, Y. Xu, R.C. Ennis, D. Fabrizio, Z.R. Chalmers, S. Balasubramanian, I. Puzanov, J.M. Balko, J.M. Cates, J.S. Ross, C. Sanders, V.A. Miller, P.J. Stephens, R.J. Sullivan, J.A. Sosman, C.M. Lovly

**Administrative, technical, or material support (i.e., reporting or organizing data, constructing databases):** D.B. Johnson, M.J. Rieth, Z.R. Chalmers, S.M. Ali, S. Balasubramanian, D.T. Frederick, I. Puzanov, J.S. Ross, J.A. Sosman

**Study supervision:** D.B. Johnson, C.M. Lovly

### Grant Support

This study was supported by ASCO Conquer Cancer Foundation Young Investigator and Career Development Awards (D.B. Johnson), NIH R01CA121210 (C.M. Lovly), Damon Runyon Clinical Investigator Award (C.M. Lovly), and American Cancer Society Professorship (J.A. Sosman).

The costs of publication of this article were defrayed in part by the payment of page charges. This article must therefore be hereby marked *advertisement* in accordance with 18 U.S.C. Section 1734 solely to indicate this fact.

Received June 27, 2016; revised August 31, 2016; accepted September 4, 2016; published OnlineFirst September 26, 2016.



## References

1. Wolchok JD. PD-1 blockers. *Cell* 2015;162:937.
2. Topalian SL, Hodi FS, Brahmer JR, Gettinger SN, Smith DC, McDermott DF, et al. Safety, activity, and immune correlates of anti-PD-1 antibody in cancer. *N Engl J Med* 2012;366:2443–54.
3. Robert C, Schachter J, Long GV, Arance A, Grob JJ, Mortier L, et al. Pembrolizumab versus ipilimumab in advanced melanoma. *N Engl J Med* 2015;372:2521–32.
4. Herbst RS, Soria JC, Kowanzet M, Fine GD, Hamid O, Gordon MS, et al. Predictive correlates of response to the anti-PD-L1 antibody MPDL3280A in cancer patients. *Nature* 2014;515:563–7.
5. Larkin J, Chiarion-Sileni V, Gonzalez R, Grob JJ, Cowey CL, Lao CD, et al. Combined nivolumab and ipilimumab or monotherapy in untreated melanoma. *N Engl J Med* 2015;373:23–34.
6. Tumei PC, Harview CL, Yearley JH, Shintaku IP, Taylor EJ, Robert L, et al. PD-1 blockade induces responses by inhibiting adaptive immune resistance. *Nature* 2014;515:568–71.
7. Snyder A, Makarov V, Merghoub T, Yuan J, Zaretsky JM, Desrichard A, et al. Genetic Basis for clinical response to CTLA-4 blockade in melanoma. *N Engl J Med* 2014;371:2189–99.
8. Van Allen EM, Miao D, Schilling B, Shukla SA, Blank C, Zimmer L, et al. Genomic correlates of response to CTLA-4 blockade in metastatic melanoma. *Science* 2015;350:207–11.
9. Rizvi NA, Hellmann MD, Snyder A, Kvistborg P, Makarov V, Havel JJ, et al. Mutational landscape determines sensitivity to PD-1 blockade in non-small cell lung cancer. *Science* 2015;348:124–8.
10. McGranahan N, Furness AJ, Rosenthal R, Ramskov S, Lyngaa R, Saini SK, et al. Clonal neoantigens elicit T cell immunoreactivity and sensitivity to immune checkpoint blockade. *Science* 2016;351:1463–9.
11. Le DT, Uram JN, Wang H, Bartlett BR, Kemberling H, Eyring AD, et al. PD-1 Blockade in tumors with mismatch-repair deficiency. *N Engl J Med* 2015;372:2509–20.
12. Johnson DB, Lovly CM, Flavin M, Panageas KS, Ayers GD, Zhao Z, et al. Impact of NRAS mutations for patients with advanced melanoma treated with immune therapies. *Cancer Immunol Res* 2015;3:288–95.
13. Peng W, Chen JQ, Liu C, Malu S, Creasy C, Tetzlaff MT, et al. Loss of PTEN promotes resistance to T cell-mediated immunotherapy. *Cancer Discov* 2015;6:202–16.
14. Spranger S, Bao R, Gajewski TF. Melanoma-intrinsic beta-catenin signalling prevents anti-tumour immunity. *Nature* 2015;523:231–5.
15. Casey SC, Tong L, Li Y, Do R, Walz S, Fitzgerald KN, et al. MYC regulates the antitumor immune response through CD47 and PD-L1. *Science* 2016;352:227–31.
16. Frampton GM, Fichtenholtz A, Otto GA, Wang K, Downing SR, He J, et al. Development and validation of a clinical cancer genomic profiling test based on massively parallel DNA sequencing. *Nat Biotechnol* 2013;31:1023–31.
17. Eisenhauer EA, Therasse P, Bogaerts J, Schwartz LH, Sargent D, Ford R, et al. New response evaluation criteria in solid tumours: revised RECIST guideline (version 1.1). *Eur J Cancer* 2009;45:228–47.
18. Gerlinger M, Quezada SA, Peggs KS, Furness AJ, Fisher R, Marafioti T, et al. Ultra-deep T-cell receptor sequencing reveals the complexity and intratumour heterogeneity of T-cell clones in renal cell carcinomas. *J Pathol* 2013;231:424–32.
19. Cancer Genome Atlas Network. Genomic classification of cutaneous melanoma. *Cell* 2015;161:1681–96.
20. Krauthammer M, Kong Y, Ha BH, Evans P, Bacchocchi A, McCusker JP, et al. Exome sequencing identifies recurrent somatic RAC1 mutations in melanoma. *Nat Genet* 2012;44:1006–14.
21. Postow MA, Luke JJ, Bluth MJ, Ramaiya N, Panageas KS, Lawrence DP, et al. Ipilimumab for patients with advanced mucosal melanoma. *Oncologist* 2013;18:726–32.
22. Luke JJ, Callahan MK, Postow MA, Romano E, Ramaiya N, Bluth M, et al. Clinical activity of ipilimumab for metastatic uveal melanoma: a retrospective review of the Dana-Farber Cancer Institute, Massachusetts General Hospital, Memorial Sloan-Kettering Cancer Center, and University Hospital of Lausanne Experience. *Cancer* 2013;119:3687–95.
23. Hugo W, Zaretsky JM, Sun L, Song C, Moreno BH, Hu-Lieskovan S, et al. Genomic and transcriptomic features of response to anti-PD-1 therapy in metastatic melanoma. *Cell* 2016;165:35–44.
24. Smith DI, Zhu Y, McAvoy S, Kuhn R. Common fragile sites, extremely large genes, neural development and cancer. *Cancer Lett* 2006;232:48–57.
25. Gubin MM, Schreiber RD. CANCER. The odds of immunotherapy success. *Science* 2015;350:158–9.
26. Hansen AR, Siu LL. PD-L1 testing in cancer: challenges in companion diagnostic development. *JAMA Oncol* 2015;1:1–2.
27. Rosenberg JE, Hoffman-Censits J, Powles T, van der Heijden MS, Balar AV, Necchi A, et al. Atezolizumab in patients with locally advanced and metastatic urothelial carcinoma who have progressed following treatment with platinum-based chemotherapy: a single-arm, multicentre, phase 2 trial. *Lancet* 2016;387:1909–20.